ELSEVIER

Physica B 304 (2001) 119–136

PHYSICA B

www.elsevier.com/locate/physb

Deep defect levels and exciton dissociation in conjugated polymers

Hsin-Fei Meng[a,*], Tzay-Ming Hong[b]

[a] *Institute of Physics, National Chiao Tung University, Hsinchu 300, Taiwan, People's Republic of China*
[b] *Department of Physics, National Tsing Hua University, Hsinchu 300, Taiwan, People's Republic of China*

Received 22 May 2000; received in revised form 30 October 2000; accepted 5 January 2001

Abstract

We study the localized deep electronic level within the bandgap of conjugated polymers in the presence of structure or oxygen (carbonyl group) defects. The structure defect is modeled as a chain twist, including the chain ends as a special case. Analytic expressions for both the energy and the wavefunction of the deep levels and the itinerant levels are obtained and supplemented by clear intuitive pictures. Carbonyl group is treated numerically within the tight-binding models. The rates of free carrier capture and exciton dissociation through the defect level via multi-phonon emission are calculated. We conclude that the defect dissociation dominates the intrinsic dissociation through thermal activation, and is the primary carrier generation mechanism in photoconductivity. Our results explain the photoconductivity enhancement due to oxidation, as well as the recent observation on the temperature-independent photocurrent in the sweep-out regime.

PACS: 72.80.Le; 73.50.Pz

Keywords: Defect levels; Exciton dissociation; Conjugated polymers

1. Introduction

One of the major differences between conjugated polymers and inorganic semiconductors is the possibility of a large exciton binding energy [1–3]. There have been controversies on how the tightly bound excitons dissociate into free carriers [1,4–7]. The carbonyl group introduced by oxidation is found to enhance the photoconductivity (PC) efficiency of poly (p-phenylene vinylene) (PPV) by a factor of 40 [8,9], suggesting that the excitons are dissociated by the carbonyl group through its defect levels. Besides, excitons can also dissociate through the surface levels at the polymer/metal junction. Barth and Bässler measured the intrinsic PC by eliminating the oxidation and junction exciton quenching [6], and concluded that in such conditions the excitons have to overcome a binding energy of 0.34 eV through

*Corresponding author. Tel.: +886-3-5731955; fax: +886-3-5720810.

E-mail addresses: meng@cc.nctu.edu.tw (Hsin-Fei Meng), ming@phys.nthu.edu.tw (Tzay-Ming Hong).

0921-4526/01/$ - see front matter
PII: S0921-4526(01)00344-1

thermal activation or electric field tunneling in order to dissociate into free carriers. The temperature and field dependence of the PC quantum yield was shown to be consistent with the Onsager model [10,6]. This picture is, however, inconsistent with the PC measurement in the sweep-out regime by Moses et al. [4] which shows that the effective activation energy decreases with the film thickness, contrary to the constant value (exciton binding energy) as the Onsager model would predict. Moses et al. thus propose that the temperature dependence of PC is mainly due to thermal activation out of the deep levels (traps) into which the carriers fall along their passage to the electrode, and the carrier generation process itself is temperature independent. This behavior is interpreted as the evidence of a small exciton binding energy [4], similar to the situation of inorganic semiconductors. Such a small binding energy is, however, difficult to reconcile with the absorption spectrum [11], as well as the recent work on the electron injection by the STM [2]. The fundamental question is then how the carriers are generated through exciton dissociation in the absence of oxidation, and why it has only a weak temperature dependence. It is well known that exciton dissociation can be mediated by the deep levels, which can be caused by not only the carbonyl group but also the unavoidable structure defects. It is generally believed that the perfect π-conjugation lasts for no more than 10 monomers [12] in conjugated polymers, while the polymer chain is as long as 1000 monomers. The π-bonding must be weakened in the conjugation interruption some way or the other, e.g. twist, by the structure defect. In addition, the chain end should also be considered as a kind of defect. Large binding energy and weak temperature dependence can be reconciled if the predominant carrier generation channel for photoconductivity is not intrinsic but mediated by such defects. The purpose of this work is to confirm this possibility by theoretical studies.

In this paper we study the properties of the electronic states in the presence of the defects, including the chain twist [13] and the carbonyl group [14], as well as the exciton dissociation process through the defect levels via multi-phonon emission. We found that the defects do introduce deep localized levels within the energy gap. For the twist case, analytical expressions are obtained for both the energy and wavefunction of the deep levels. The scattering of the itinerant states by the defect is also considered. In practice, whether the defect is actually a rotation or other fault is not critical because such bond weakening is the sole assumption in our calculation on the deep level. Such deep level is strongly coupled to the local phonon mode centered around the defect because of the large wavefunction overlap. The local phonon mode is displaced to a new equilibrium position once the electron drops into the deep level from the conduction band. When the level is initially empty, the electron of the exciton can be captured by the deep level while releasing the hole into a free carrier, assuming the defect binding energy is larger than the exciton binding energy. The reversed process happens when the level is initially empty. This is a relaxation instead of activation process. Carriers can therefore be generated almost independent of the temperature.

The dissociation through structure defects is found to be the predominant carrier generation process at a typical density level of the structure defects. The temperature independence of the photocurrent is not due to the smallness of exciton binding energy, but the high quenching efficiency of the deep levels. From the exciton capture rate we calculate the steady state PC quantum yield, i.e. the number of carriers per absorbed photon. As expected, the quantum yield decreases with the light intensity because the carrier generation process is blocked when the defect levels are saturated by high photoexcitation. Similar behavior has been, in fact, suggested by the two-pump experiments [15]. These results provide a unifying picture for the PC experiments [4,6] and clarify the controversy on the origin of the photocarrier generation process.

In Section 2, we introduce the model Hamiltonian with a single twisted bond (structure defect), and derive the expressions for the energy and wavefunction of the electronic states. In Section 3, we calculate the energy and wavefunctions of the localized states around the oxygen defect

numerically. In Section 4, we calculate the free carrier capture rate through the defect. In Section 5, we generalize the case of exciton dissociation (carrier generation). In Section 6, the PC quantum yield is calculated as a function of photon flux and defect density. Finally, Section 7 is devoted to discussion and conclusion.

2. Structure defects

2.1. Perfect chain

The π-electrons in one chain of conjugated polymer is described by the many-body Hamiltonian $H = H_f + H_c$, where H_f is the free part including the kinetic energy and the periodic potential, and H_c is the Coulomb interaction among the π-electrons. In the Hartree–Fock (HF) self-consistent field (SCF) approximation, the ground state $|g\rangle$ is a Slater determinant made up of the single-particle wavefunctions determined by the self-consistent Hartree–Fock operator H^{SCF} [16]. On the basis of the $2p_z$ orbitals $\psi_\mu(\mathbf{r})$ at the carbon sites labeled by μ, H^{SCF} is further approximated by the Su–Schrieffer–Heeger model [17] as a one-dimensional infinite lattice with alternating values of hopping integrals t_1 and t_2 between the neighboring $2p_z$ orbitals:

$$H^0 \equiv H^{SCF} = \sum_n t_1 c^\dagger_{2n-1} c_{2n} + t_2 c^\dagger_{2n} c_{2n+1},$$

where $t_1(t_2)$ denotes the hopping matrix element on a single (double) bond and $|t_2|$ is bigger than $|t_1|$. $c^\dagger_\mu$ and c_μ are the creation and annihilation operators of the $2p_z$ orbitals, respectively. n labels the repeat unit which contains two carbon atoms. Spin indices are neglected for simplicity. For conjugated polymers with more complicated repeat unit like PPV, t_1 and t_2 can be taken as parameters which reproduce the conduction and valence band structures. Even though the Hamiltonian H^0 is for single-particle states, the Coulomb interaction among the π-electrons have been included self-consistently by choosing the renormalized values for the hopping integrals. The single-particle energy spectrum of H^0 is denoted by E^0_i with corresponding wavefunction ϕ^i, whose component at site μ is ϕ^i_μ, $i = 1, 2, \ldots, N$, where N is the total number of carbon atoms in the chain. The ground state energy E_g of the many-body system is given by $E_g = \langle g|H|g\rangle = 2\sum_{E^0_i < E_F} E^0_i$. The Fermi level E_F is controlled by the total number of π-electrons. For the perfect chain it is equal to N, so half of the levels are filled due to spin degeneracy. This approximation applies to chains with defects as well for which the number of electrons may be different from the number of carbon atoms as discussed below. An electron–hole pair state is created when one electron below E_F is promoted above E_F. Configuration interaction (CI) among such states due to Coulomb interaction must be considered in order to obtain the excited state of the many-body system. This will be the subject of Section 5 where exciton dissociation is discussed. The electron–phonon coupling is introduced in Section 6 in order to study the carrier capture through multi-phonon emission.

For convenience, the components $\phi_{k,\mu}$ of the eigenfunction with crystal momentum k at the even and odd sites will be denoted, respectively, by $Ve^{ik(2n+1)}$ for $\mu = 2n+1$ and $u_n = Ue^{ik2n}$ for $\mu = 2n$ (see Fig. 1). It is easy to show that the spectrum consists of two bands.

$$E^\pm_k = \pm\sqrt{t_1^2 + t_2^2 + 2t_1 t_2 \cos 2k} \equiv \pm\bar{t}_k \tag{1}$$

and

$$U/V = e^{\pm i\theta} \quad \text{where} \quad \tan\theta = \frac{(t_1 - t_2)}{(t_1 + t_2)}\tan k. \tag{2}$$

k is in the unit of inverse lattice constant. The valence band is between $-|t_1 + t_2|$ and $-|t_1 - t_2|$, while the conduction band between $|t_1 - t_2|$ and $|t_1 + t_2|$. The direct bandgap is located at Brillouin zone boundary $k = \pi/2$. Therefore $E^0_i \to E^-_k$, $\phi^i_\mu \to \phi^-_{k,\mu}$ below E_F; and $E^0_i \to E^+_k$, $\phi^i_\mu \to \phi^+_{k,\mu}$ above

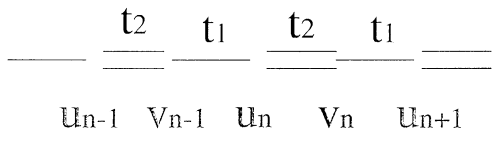

Fig. 1. A perfect chain consists of alternating bonds t_1 and t_2. n labels the unit cell with two p_z orbitals. u_n and v_n are the components of the wavefunction at the two orbitals.

E_F. The real-space wavefunction for the eigenstates of the electrons are $\psi_{c,k}(\mathbf{r}) = \sum_\mu \phi^+_{k,\mu}\psi_\mu(\mathbf{r})$ and $\psi_{v,k}(\mathbf{r}) = \sum_\mu \phi^-_{k,\mu}\psi_\mu(\mathbf{r})\cdot$ $c(v)$ indicates conduction (valence) band.

We are interested in how defects affect the energy levels and, in particular, searching for new localized states within the bandgap. For this reason, it is important to note first that an open boundary condition can introduce localized states centering about any weak bond in the chain end. This result is independent of the size of the polymer, i.e., it exists even in the thermodynamic limit. When only one end belongs to the weak bond, this localized state has zero energy. This is expected for a Hamiltonian with electron–hole symmetry when there are odd number of sites (and degrees of freedom). It is less obvious, but can be easily confirmed numerically, that when both ends are weak bonds they give rise to two localized states with energies $\pm E^*$ where E^* is nonzero but much less than the bandgap, $2|t_2 - t_1|$. Since real polymers are open in boundary, these localized states will be relevant to our studies of the optical properties. However, to avoid confusion, periodic boundary condition will be used when we analyze the effects of other defects from now on, and chain boundary is included by studying a periodic chain with one bond broken as below.

2.2. Chain with one defect

The structure defect is introduced by changing the value of one of the hopping integrals, which we call t_1 without the loss of generality, by Δt. Physically a negative Δt can be caused by chain twist or distortion, which reduces the p_z orbital overlap. Our consideration applies, however, to a positive Δt as well. Chain boundary can also be included by setting $\Delta t = -t_1$, in such case the hopping is zero and the π-electron conjugation is completely interrupted. Assume the defect occurs at the bond between site p and $p+1$. One common defect is the twisting of polymers such that the local hopping amplitude gets decreased. As will be shown in the next section, the consequence is very different depending on whether it is a single or double bond that gets modified. But the general approach is to first express the Schrödinger equation for the perfect chain in the matrix form: $\sum_v L_{\mu v}\phi^i_v \equiv E^0_i\phi^i_\mu - \sum_v H^0_{\mu v}\phi^i_v = 0$ where v is the site label and i distinguishes the different unperturbed eigenfunctions ϕ^i and eigenvalues E^0_i. It is easy to show that

$$H^0_{\mu v} = \frac{1}{N}\sum_i E^0_i \phi^{i*}_\mu \phi^i_v \tag{3}$$

from the completeness relation $\sum_i \phi^{i*}_\mu \phi^i_v = N\delta_{\mu v}$. The Schrödinger equation can be abbreviated as $\mathbf{L}\phi = 0$. With defects, the equation becomes $(\mathbf{L} + \delta\mathbf{L})\psi = 0$ where $L_{\mu v} \equiv E\delta_{\mu v} - H^0_{\mu v} = (1/N)\sum_i (E - E^0_i)\phi^{i*}_\mu \phi^i_v$ because of Eq. (3). ψ is the new wavefunction with the defect, whose component at site v is indicated by ψ_v below. One crucial step here is to rewrite [18][1] it as

$$(1 + \mathbf{L}^{-1}\delta\mathbf{L})\psi = 0, \tag{4}$$

where $\mathbf{L}^{-1}$ plays the role of bare electron propagator and can be read off from the expression for $L_{\mu v}$ as

$$L^{-1}_{\mu v} = \frac{1}{N}\sum_i \frac{1}{E - E^0_i}\phi^{i*}_\mu \phi^i_v. \tag{5}$$

Note that this approach and the transfer matrix formulation are common in considering $\mathbf{L}^{-1} = (E - H_0)^{-1}$ as the Green's function, where H_0 is the Hamiltonian without the defect. The Schrödinger equation with the defect $-\delta\mathbf{L}$ is then written as $(\mathbf{1} + \mathbf{L}^{-1}\delta\mathbf{L})\psi = 0$ in our approach, while it is written as $\psi = -\mathbf{L}^{-1}\delta\mathbf{L}\psi + \phi$ in transfer-matrix formulation, where ϕ is the eigenstate of H_0. They differ in that ψ is usually solved perturbatively in $\delta\mathbf{L}$ in the transfermatrix formulation by taking $\mathbf{L}^{-1}$ as the integral kernel, while we happen to be able to solve the problem exactly without the infinite series expansion.

Let the twist in a polymer change the hopping amplitude t_1 to $t_1 + \Delta t$ between sites p and $p+1$, then

$$\delta L_{\mu v} = \Delta t[\delta_{\mu,p}\delta_{v,p+1} + \delta_{\mu,p+1}\delta_{v,p}]. \tag{6}$$

[1] Same procedures are found in the discussions of eigenmodes for a series of springs with defects in Ref. [18].

The pth and $(p+1)$th components of Eq. (4) are

$$\psi_p + \Delta t L^{-1}_{p,p}\psi_{p+1} + \Delta t L^{-1}_{p,p+1}\psi_p = 0,$$
$$\psi_{p+1} + \Delta t L^{-1}_{p+1,p}\psi_{p+1} + \Delta t L^{-1}_{p+1,p+1}\psi_p = 0. \quad (7)$$

The existence of nontrivial ψ_p and ψ_{p+1} requires the determinant composed by their coefficients in Eq. (7) to equal zero, by which equation the new eigenenergies can then be determined:

$$\frac{1}{\Delta t} = \sum_k \left[\frac{1}{E-\bar{t}_k}(e^{i\theta}e^{ipk})(e^{i(p+1)k})^* + \frac{1}{E+\bar{t}_k}(e^{i\theta}e^{ipk})(-e^{i(p+1)k})^*\right] \pm \sum_k \left[\frac{1}{E-\bar{t}_k}(e^{i\theta}e^{ipk})(e^{i\theta}e^{ipk})^* + \frac{1}{E+\bar{t}_k}(e^{i\theta}e^{ipk})(e^{i\theta}e^{ipk})^*\right] = \sum_k \frac{2\bar{t}_k\cos(\theta-k) \pm 2E}{E^2-(\bar{t}_k)^2}, \quad (8)$$

where $\bar{t}_k$ and θ_k are defined in Eqs. (1) and (2). If it is t_2 that gets modified, all we need to do is to interchange the label of t_1 and t_2. The electron–hole symmetry is indeed exhibited in Eq. (8) that $-E$ will be a solution if E is a solution. For simplicity, we shall limit ourselves to the discussion of the plus case in Eq. (8).

2.3. Localized states

All states with energy not falling into the existing two bands are localized. Let us first study the special case of $E=0$. This is of particular interest since the conjugated polymers are semiconducting and their Fermi level lies close to the middle of the bandgap at low temperatures. Setting $E=0$, Eq. (8) reduces to

$$\frac{1}{\Delta t} = \frac{1}{2t_1}\left(\frac{t_1^2-t_2^2}{|t_2^2-t_1^2|}+1\right) = \begin{cases} 0 & \text{if } t_1^2 < t_2^2, \\ -\dfrac{1}{t_1} & \text{if } t_1^2 > t_2^2. \end{cases} \quad (9)$$

This tells us that the zero-energy modes occur at $\Delta t \to \pm\infty$ when it is a weak bond that gets twisted. The second case is expected from the boundary effects discussed in the previous section because $\Delta t = -t_1$ cuts the polymer into two separate segments and expose two new ends with weak bonds. In general, if E lies either above the conduction band or below the valence band, Eq. (8) can be simplified to

$$\frac{1}{\Delta t} = -\frac{1}{2t_1}\times\left\{1-\sqrt{\frac{[E+(t_1+t_2)][E-(t_2-t_1)]}{[E-(t_1+t_2)][E+(t_2-t_1)]}}\right\}. \quad (10)$$

This equation also applies when E lies within the bandgap if $t_1^2 < t_2^2$. But for $t_1^2 > t_2^2$, the minus sign before the square root needs to be changed into plus. It is easy to check that Eq. (9) is consistent with the general formula above. The relation between $1/\Delta t$ and E is shown in Fig. 2. Localized states within the bandgap are introduced by the defect when $-2t_1/\Delta t < 1$ for $t_2 > t_1$, and $-2t_1/\Delta t > 1$ for $t_2 < t_1$. This relation can be converted to obtain E as a function of Δt. The result is that the defect level energy E_d, appearing in pairs of the same magnitude but opposite sign, is given by

$$E_d^{\pm} = \pm\frac{t_1(1+A)-\sqrt{4t_1^2A+t_2^2(A-1)^2}}{(A-1)}, \quad (11)$$

where $A \equiv ((2t_1/\Delta t)+1)^2$. For the localized states outside the energy bands, the expression becomes $E^{\pm}_{d,\mathrm{out}} = \pm[t_1(1+A)+\sqrt{4t_1^2A+t_2^2(A-1)^2}]/(A-1)$.

The amplitudes of these localized states can be obtained by solving Eq. (4) for a general q-component:

$$\frac{\psi_q}{\psi_p} = \Delta t\sum_k\left[\frac{2E}{E^2-(\bar{t}_k)^2}e^{i(q-p)k} + \frac{2\bar{t}_k}{E^2-(\bar{t}_k)^2}e^{i\theta}e^{i(q-p-1)k}\right] \quad (12)$$

when q belongs to the u sites (denoted in Fig. 1), and

$$\frac{\psi_q}{\psi_p} = \Delta t\sum_k\left[\frac{2E}{E^2-(\bar{t}_k)^2}e^{i(q-p-1)k} + \frac{2\bar{t}_k}{E^2-(\bar{t}_k)^2}e^{-i\theta}e^{i(q-p)k}\right] \quad (13)$$

for the v sites. The exponentially decaying behaviour of ψ_q is due to the cancellation of the rapidly oscillating function $e^{i(q-p)k}$. For completeness, their final expressions after the summation are

$$\frac{\psi_q}{\psi_p} = \frac{\Delta t}{E^2 - t_1^2 - t_2^2}\left\{ \frac{E}{\sqrt{1-B^2}}\left[\frac{\sqrt{1-B^2}-1}{B}\right]^{q-p/2} + \frac{t_1}{\sqrt{1-B^2}}\left[\frac{\sqrt{1-B^2}-1}{B}\right]^{q-p/2} + \frac{t_2}{\sqrt{1-B^2}}\left[\frac{\sqrt{1-B^2}-1}{B}\right]^{(q-p/2)-1}\right\} \quad (14)$$

for q in the u sites where $B \equiv -2t_1t_2/E - t_1^2 - t_2^2$, and

$$\frac{\psi_q}{\psi_p} = \frac{-\Delta t}{-E^2 + t_1^2 + t_2^2} \times \left\{ \frac{E}{\sqrt{1-B^2}}\left[\frac{\sqrt{1-B^2}-1}{B}\right]^{q-p-1/2} + \frac{t_1}{\sqrt{1-B^2}}\left[\frac{\sqrt{1-B^2}-1}{B}\right]^{q-p-1/2} + \frac{t_2}{\sqrt{1-B^2}}\left[\frac{\sqrt{1-B^2}-1}{B}\right]^{q-p+1/2}\right\} \quad (15)$$

for the v sites.

2.4. Physical pictures

We shall now provide simple physical pictures for the seemingly complicated results in Eq. (10). Using the language of renormalization group, $t_1 = t_2$ is expected to mark a dramatic change of fixed points when approached from either $t_1 > t_2$ or $t_1 < t_2$ (when there is a bandgap). Of course, it is not known a priori whether there is any further phase transition before hitting $t_1 = t_2$. But, this has been checked and ruled out by our calculations. So, it is safe to turn off the weak hoping t_1 first, which leaves us with independent double bonds whose eigenenergies are simply $\pm t_2$ for the bonding and antibonding states. Consider the twisting to occur in a weak bond, and denote the resulting hopping amplitude $t_1 + \Delta t_1$ by t_1'. It connects two neighboring double bonds (Fig. 3) and gives four new states (Fig. 4) with energy E satisfying

$$\det\begin{vmatrix} -E & t_2 & 0 & 0 \\ t_2 & -E & t_1' & 0 \\ 0 & t_1' & -E & t_2 \\ 0 & 0 & t_2 & -E \end{vmatrix} = 0.$$

When t_1 is turned on, it broadens the $\pm t_2$ levels into bands with width $\approx 2|t_1|$ and turns all the levels within its range into itinerant states (see Fig. 4). It becomes clear from the figure why Eq. (9) requires the zero-energy states to occur at $\Delta t_1 = \pm\infty$. Since twisting tends to decrease the electron hopping amplitude, i.e. $|t_1'| \leqslant |t_1|$, there will be *no localized states* either close to the Fermi level in the gap or outside of the two bands.

Let us now consider the twisting to be at a double bond (with a new hopping t_2'). In the absence of t_1, we have two bonding and two antibonding states at energies $\pm t_2$ and $\pm t_2'$ (Fig. 5). Turning on t_1 again broadens the $\pm t_2$ levels into bands, and turns parts of the $\pm t_2'$ within its range into itinerant states (Fig. 5). The number of states and their dependence on the defect hopping amplitude are very different in Figs. 5 and 6. The twisting causes $|t_2'| \leqslant |t_2|$ and now allows for two mid-gap states. In contrast to the t_1' case, this is *relevant* to the optical properties of conjugated polymers.

2.5. Itinerant states

It is worth mentioning that we need to put in the unperturbed part, $\phi(k)$, when calculating the wavefunction amplitudes of an itinerant state from Eq. (4). That is,

$$\psi_q(k) = \phi_q(k) - L_{q,p}^{-1}\delta L_{p,p+1}\psi_{p+1}(k) - L_{q,p+1}^{-1}\delta L_{p+1,p}\psi_p(k). \quad (16)$$

This is a standard procedure in the perturbation theory. The correction to $\phi_q(k)$ can be worked out to all orders of Δt by self-consistently substituting the right-hand side into $\psi_{p+1}(k)$ and $\psi_p(k)$. When Δt modifies the weak bond, we obtain

to the first order in Δt

$$\psi_q(k) = e^{i\theta}e^{ikq} + \frac{\Delta t \qquad e^{ikp}}{E^2 - t_1^2 - t_2^2\sqrt{B^2-1}} \times \left\{ \pm e^{ik} E \sin\left(\frac{q-p}{2}\eta\right). + e^{i\theta}\left[t_1 \sin\left(\frac{q-p}{2}\eta\right). + t_2 \sin\left(\frac{q-p-2}{2}\eta\right)\right]\right\} \quad (17)$$

for q in the u sites. The plus (minus) sign is for the conduction (valence) band, $B \equiv -2t_1t_2/(E - t_1^2 - t_2^2)$, and $\cos\eta \equiv -1/B$ and $\sin\eta \equiv \sqrt{B^2-1}/B$. When q is in the v sites,

$$\psi_q(k) = \pm e^{ikq} + \frac{\Delta t \qquad e^{ikp}}{E^2 - t_1^2 - t_2^2\sqrt{B^2-1}} \times \left\{ \pm e^{ik} E \sin\left(\frac{q-p-1}{2}\eta\right) + e^{i\theta}\left[t_1 \sin\left(\frac{q-p-1}{2}\eta\right) + t_2 \sin\left(\frac{q-p-1}{2}\eta\right)\right]\right\}. \quad (18)$$

As before, interchange the labels of t_1 and t_2 when Δt occurs at a double bond.

3. Oxygen defect (carbonyl group)

Another common type of defect is the substitution of an oxygen for a hydrogen atom (the carbonyl group), resulting from oxidation. The oxygen atom is attached to one of the carbon atoms with a double bond. That carbon atom has therefore a single bond on each of the two sides. In order to keep the difference between the bonding structure of oxidized chain and perfect chain local, an extra hydrogen atom is usually attached to the carbon atom right next to the one bonded to the oxygen, such that it is bonded to four neighboring atoms (two hydrogens and two carbons) with sp^3 hybridization. The structure of the oxidized chain is shown in Fig. 6. Each of the atomic orbitals contributing to the π-conjugation is labeled by a number. Note that the bonding beyond site 1 and 8 is exactly the same as the unoxidized case. Among the four sp^3 orbitals of carbon, only two of them (sites 4,5) are roughly perpendicular to the sp^2 plan (x–y plane) and participate in the π-electron wavefunction. Each of them are bonded to the 1s orbital of an hydrogen atom. In addition, they also overlap with the p_z orbitals of the neighboring carbon atoms. Such overlap is sometimes termed hyperconjugation [22], because the resulting wavefunction is a mixture of sp^3 and sp^2+p_z hybridization. The off-diagonal matrix elements of the Hamiltonian among the atomic orbitals around the oxygen defect are summarized by $t_{23} = t_O$, $t_{24} = t_{48} = -t_{25} = -t_{58} = t_h$, $t_{57} = t_{46} = t_H$, where t_O is the hopping between carbon 2 and the oxygen (site 3), t_h is the hopping for hyperconjugation, and t_H is the hopping between hydrogen 1s to the carbon sp^3 orbital (sites 4,5). We choose $t_h = \frac{1}{2}\cos(\phi)t_2$, where t_2 is the single bond hopping same as the structure defect considered above. $\phi = 25.16^\circ$ is the angle between the tetrahedral sp^3 bonds and the neighboring p_z orbital. t_{ij} is equal to t_{ji} by symmetry. As for the diagonal matrix element of the Hamiltonian, i.e., the on-site energy, we choose $\varepsilon_H = 0$ for hydrogen because the hydrocarbon bond is known to be covalent. The negative chemical potential ε_O describes the tendency for the oxygen defect (site 3) attract electrons, but whether this is strong enough to induce localized states within the bandgap is our primary concern. The block of the matrix Hamiltonian **H** around the oxygen (site 3) becomes

$$\mathbf{H} = \begin{pmatrix} 0 & t_1 & 0 & 0 & 0 & 0 & 0 & 0 \\ t_1 & 0 & t_O & t_h & -t_h & 0 & 0 & 0 \\ 0 & t_O & \varepsilon_O & 0 & 0 & 0 & 0 & 0 \\ 0 & t_h & 0 & 0 & 0 & t_H & 0 & t_h \\ 0 & -t_h & 0 & 0 & 0 & 0 & t_H & -t_h \\ 0 & 0 & 0 & t_H & 0 & 0 & 0 & 0 \\ 0 & 0 & 0 & 0 & t_H & 0 & 0 & 0 \\ 0 & 0 & 0 & t_h & -t_h & 0 & 0 & 0 \end{pmatrix}. \quad (19)$$

Outside this 8×8 block, the matrix is the same as a perfect chain of alternating bonds. The parameters for PPV are used here [22]: $t_O = -2.9$ eV,

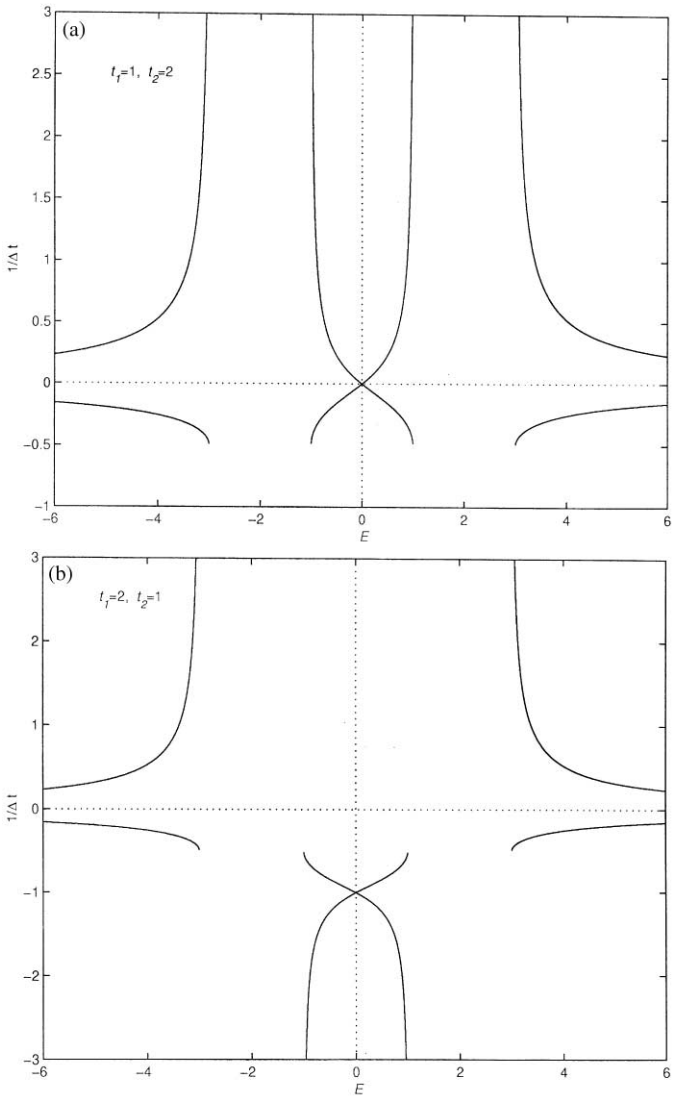

Fig. 2. The relation between the inverse change $1/\Delta t$ of one t_1 bond and the deep level energy E in Eq. (10) is plotted for $t_1 = 1,\ t_2 = 2$ (a); and $t_1 = 2,\ t_2 = 1$ (b). We take $t_{1,2}$ to be positive integers temporarily for simplicity.

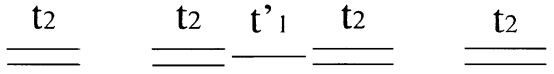

Fig. 3. All the single bonds t_1 are turned off, except for the twisted bond t_1'.

$t_1 = -1.5$ eV, $t_2 = -2.9$ eV, $t_H = -4$ eV, $t_h = -1.2$ eV, and $\varepsilon_O = 2t_1$. Analytic expressions energies and wavefunctions of the localized states for an infinite chain in this case are quite involved, and so we proceed with the numerical diagonalization of a finite matrix containing the carbonyl group. It turns out that the results remain the same as long as the chain contains more than about 40 carbon atoms. We found that there are two localized states. One is below the valence band with predominant weighting on the oxygen atom (oxygen level). Another one is inside the gap (deep level), which is responsible for the carrier capture. Since each of the atomic orbitals contributes one

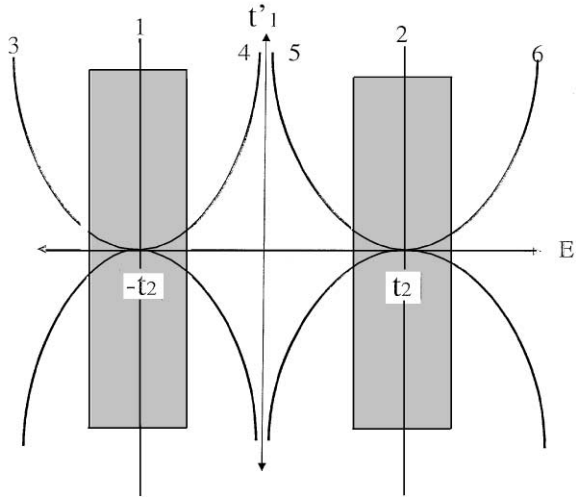

Fig. 4. The situation of a twisted single bond is illustrated. When all the single bonds t_1 are turned off, the energy $\pm t_2$ (denoted as 1 and 2) are infinitely degenerate. When the defect bond t_1' is turned on, four extra nondegenerate states (denoted as 3, 4, 5 and 6) occur. When all the rest of the single bonds t_1 are turned on, 1 and 2 are broadened into bands of width $2|t_1|$ (gray area). When t_1' is too weak, the nondegenerate states are covered by the bands and absorbed into the continuum of itinerant states. Localized state exists only when t_1' is large enough such that the nondegenerate state remain outside the gray area.

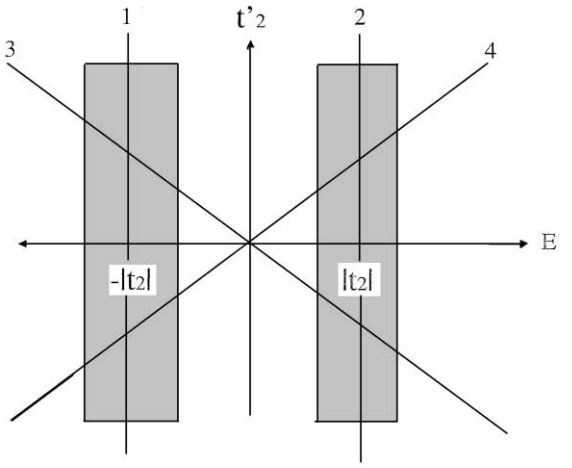

Fig. 5. The situation of a twisted double bond is illustrated. When all the single bond t_1 is turned off and the defect double bond t_2' is turned on, two extra nondegenerate states (denoted as 3, and 4) occur, in addition to the infinitely degenerate states 1 and 2. When all the single bonds t_1 are turned on, 1 and 2 are broadened into bands of width $2|t_1|$ (gray area). Since $|t_1|$ is smaller than $|t_2|$, the nondegerate state near $E = 0$ will never be absorbed into the gray area to become an itinerant state. So two localized states always occur in this situation.

π-electron, the Fermi level can be obtained by filling the states from below. It turns out to be between the valence band and the deep level. The energy of the deep level is located at $\varepsilon_d = 0.78$ eV (the bandgap is from -1.4 to 1.4 eV) whose wavefunction, as shown in Fig. 7, is localized around the oxygen and spreads out to about five sites on each side.

4. Electron–phonon coupling and free carrier capture

Now we consider the capture of free carriers by the deep level through multi-phonon emission. The structure defect can produce both localized electronic state and localized phonon mode, represented as a simple harmonic oscillator, with strong coupling between them due to the large wavefunction overlap. In other words, the electronic energy is a function of the lattice displacement. The total energy of the system is then the electronic energy plus the lattice distortion energy. The position of the harmonic oscillator that minimizes the total energy therefore depends on whether the electronic level is filled or empty. The harmonic oscillator is displaced when the electron drops from a free state, with a negligible electron–phonon coupling, to the deep level. The capture rate P_k for a free electron with momentum k is determined by the nonadiabatic (NA) part of the Hamiltonian [20,21]

$$P_k = \frac{2\pi}{\hbar^2\omega}\mathrm{Av}_m|\langle\Psi_k,\chi_{k,m}|H^{\mathrm{NA}}|\Psi_d,\chi_{k,m+p}\rangle|^2 = 2\pi\omega\left|\langle\Psi_k|\frac{\partial}{\partial Q}|\Psi_d\rangle_{Q^*}\right|^2 I_k(p), \quad (20)$$

where $\Psi_{k,d}$ and $\chi_{k,d}$ are the wavefunctions for the electronic and the lattice parts, respectively. k and d each labels the free and defect states. ω is the angular frequency of the local phonon mode, and Q is the dimensionless normal coordinate of the local phonon mode. "Av_m" denotes thermal average over the initial phonon number m. The minimum of total energy is at $Q = 0$ when the

electron is free, and at Q^* when the electron is captured. $p \equiv (E_k - E_d)/\hbar\omega$ is the number of phonons emitted, where E_k and E_d are the total energy for the initial (free) and final (captured) states, In the low temperature limit where $\hbar\omega\beta \gg 1$, the lattice factor $I_k(p)$ is given by

$$I_k(p) = \left(\sqrt{\frac{p}{2}}F_{0,p-1} + \sqrt{\frac{p+1}{2}}F_{0,p+1}\right)^2. \qquad (21)$$

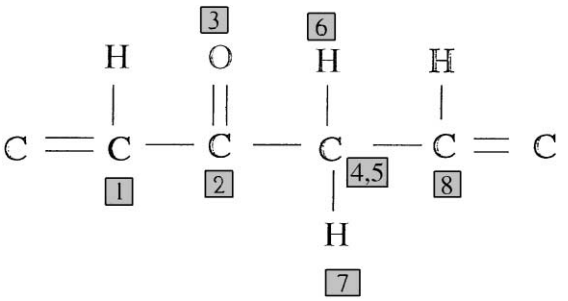

Fig. 6. The atomic orbitals included in the tight binding calculation are labeled by their site numbers.

$F_{m,m+p}$ is the overlap between two displaced harmonic oscillators with quantum numbers m and $m+p$. Explicitly we have [20,21] $F_{0,p} = (-\sqrt{S})^p e^{-S/2}/\sqrt{p!}$ where $S \equiv \frac{1}{2}Q^{*2}$ is the Huang–Rys factor. In order to calculate the capture rate, we need to know the Q-dependence of both the localized electron energy $\varepsilon_d(Q)$ and wavefunction $\Psi_d(Q)$. In the following we make an approximation by assuming that the coupling of the local phonon mode to the electron is mostly through the modulation of the defect bond, i.e. the bond between sites p and $p+1$. Even though the local phonon mode may extend for several lattice constants, this is a reasonable approximation because both the electron and phonon wavefunctions are highly localized around the same defect bond. We therefore write $\Delta t(Q) = \Delta t_0 + \eta Q$, where Δt_0 is due to the permanent bond twist at the defect, and ηQ is due to the bond oscillation. The constant η depends on the nature of the defect and will be specified later. The Hamiltonian can be expressed as $H(Q) = H_0 + VQ$ with $V_{\mu,\nu} = \eta(\delta_{\mu,p}\delta_{\nu,p+1} + \delta_{\nu,p}\delta_{\mu,p+1})$. To the first order in Q,

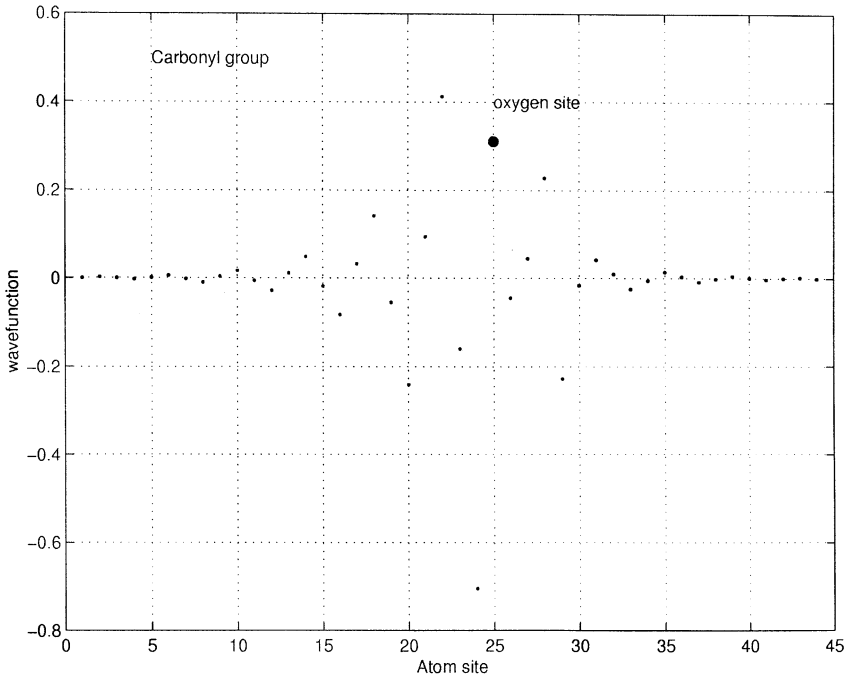

Fig. 7. The normalized wavefunction of the localized deep level within the bandgap caused by the carbonyl group is shown. The site of the oxygen atom is highlighted. The wavefunction extends for about five unit cells.

the energy of the defect level $E_d(Q)$ is

$$E_d(Q) = E_d(0) + \langle \Psi_d(0)|VQ|\Psi_d(0)\rangle = E_d(0) + \eta Q(\psi^*_{d,p}\psi_{d,p+1} + \psi^*_{d,p+1}\psi_{d,p}), \quad (22)$$

where $\psi_{d,p}$ is the component of the localized electronic state Ψ_d at site p for $Q = 0$. The total energy of the system is then

$$E_t(Q) = E_d(Q) + \tfrac{1}{2}\hbar\omega Q^2. \quad (23)$$

The harmonic oscillator is displaced to the new minimum E_t^* of $E_t(Q)$ at Q^*. Similarly the wavefunction can be expanded to the first order in Q by

$$|\Psi_d(Q)\rangle = Q\sum_m \frac{\langle m|V|\Psi_d\rangle}{E_d - E_m}|m\rangle, \quad (24)$$

where $|m\rangle$ is the other eigenstate of H_0. The nonadiabatic matrix element is

$$\langle \Psi_k|\frac{\partial}{\partial Q}|\Psi_d\rangle_{Q^*} = \frac{\eta(\psi^*_{k,p}\psi_{d,p+1} + \psi^*_{k,p+1}\psi_{d,p})}{E_d - E_k}. \quad (25)$$

For the conduction band state Ψ_k, the components $\psi_{k,p}$ and $\psi_{k,p+1}$ are always equal due to the inversion symmetry. So we approximate them by $1/\sqrt{N}$, where N is the total number of sites. The matrix element becomes

$$\langle \Psi_k|\frac{\partial}{\partial Q}|\Psi_d\rangle_{Q^*} = \frac{1}{\sqrt{N}}\eta\frac{(\psi_{d,p+1} + \psi_{d,p})}{E_d - E_k}. \quad (26)$$

Note that the factor $1/\sqrt{N}$ ensures $P_k \sim 1/N$ as $N \to \infty$ for one single defect as it should be. In practice, the number of defects is also proportional to N such that the capture rate is finite as $N \to \infty$.

4.1. Chain twist

If the bond t_1 is twisted by an angle θ permanently, the parameters above are given by

$$\Delta t_0 = t_1[1 - \cos(\theta)], \qquad \eta = 2\psi_p\alpha\cos(\theta)\sqrt{\frac{\hbar}{M\omega}}. \quad (27)$$

M is the atom mass of carbon and $\alpha = \mathrm{d}t_1/\mathrm{d}l$, where $l = \sqrt{\hbar/M\omega}\psi_{d,p}Q$ is the change of bond length due to the normal mode coordinate Q. Here we have assumed that the local mode profile follows the electronic wavefunction. The reason is that the very existence of the local phonon mode itself is due to the localization of electron and the electron–lattice coupling, while neglecting any local change in the force constant for the bond oscillation.

4.2. Chain end

Let us consider another kind of structure defect: the end of a semi-infinite chain composed of sites with index smaller or equal to p. Localized electronic and phonon mode occur simultaneously at the end. For the electronic part, we can set Δt equal to $-t_1$, such that the hopping is zero between sites p and $p+1$. The deep level is then located at $E = 0$. The local phonon mode is still assumed to follow the electron wavefunction. The coupling between the local mode and the electron is approximated to be through the modulation of the last bond between sites $p-1$ and p. The Q-dependent part of the Hamiltonian is then $V_{\mu,\nu}Q = Q\eta(\delta_{\mu,p}\delta_{\nu,p-1} + \delta_{\nu,p}\delta_{\mu,p-1})$. Again the conduction band state is always in phase at the last two sites of the chain. So we have

$$E_d(Q) = \eta 2Q\psi_{d,p}\psi_{d,p+1},$$
$$\langle \Psi_k|\frac{\partial}{\partial Q}|\Psi_d\rangle_{Q^*} = \frac{1}{\sqrt{N}}\eta\frac{(\psi_{d,p-1} + \psi_{d,p})}{E_d - E_k}, \quad (28)$$

with $\eta = 2\psi_p\alpha\sqrt{\hbar/M\omega}$.

4.3. Oxygen

The obvious local phonon mode strongly coupled to the localized electron level is the oscillation of the C = O double bond. The energy $E_d(Q)$ of the deep level is calculated numerically by assuming $\Delta t_O = \alpha\sqrt{\hbar/M_r\omega_O}Q$, where M_r is the reduced mass and ω_O is the angular frequency of the oscillation.

4.4. Result

We define for convenience the capture rate $1/\tau^f \equiv P_f N_c$, where $N_c = N/2$ is the number of unit cells. τ^f is the carrier capture lifetime when there is on average one defect per unit cell. It has the advantage of being independent of the system size. For a chain with N_d defects, the capture rate

is $P_k N_d = n_d/\tau_1$, where $n_d = N_d/N_c$ is the number of defect per cell, or the defect density.

For the twist case, the empty defect energy E_d in Eq. (11) ("+" is omitted) and the defect wavefunction $\psi_{d,p(p+1)}$ in Eq. (14) are inserted into Eq. (25) to obtain the NA matrix element. For the oxygen case, the defect energy and the wavefunction are obtained from the numerical results in Figs. 8 and 7, respectively. After numerical differentiation $\partial/\partial Q|\Psi_d\rangle_{Q^*}$ of the wavefunction, we calculate its inner product with the free state $|\Psi_k\rangle$ to get the NA matrix element $\langle\Psi_k|\partial/\partial Q|\Psi_d\rangle_{Q^*}$. The result is shown in Fig. 9. The Huang–Rys factor $S = Q^{*2}/2$ is obtained from Eqs. (22) and (23). S is then inserted into Eq. (21) to get the lattice factor I_p. The NA matrix element and the lattice factor are then inserted into Eq. (20) to get the final result of the capture rate P_k, which is shown in Fig. 10. As in Section 3, we choose $t_1 = -2.9$ eV [11] and $t_2 = -1.5$ eV, suitable for PPV with bandgap believed to be near 2.8 eV [23]. The values of α and $\hbar\omega_0$ are 4.1 eV/Å [17] and 0.18 eV for the C=C bond, and 3.5 eV/Å and 0.17 eV for the C=O bond [9], respectively. The reduced mass for C=C bond is used for local mode around the twisted bond, while the reduced mass for C=O is used for the oxygen case.

5. Coulomb interaction and exciton dissociation

Excitons, i.e. bound states of one electron and one hold, are the elementary excited states of semiconductors created by either optical or electric excitation. Excitons can recombine nonradiatively through the deep level defects discussed above. In the Hartree–Fock approximation considered in Section 2, we obtained the self-consistent single-particle states with energy $E_k^{\pm}$ for the valence and conduction bands, respectively. In the ground state $|g\rangle$ the valence band is filled and the

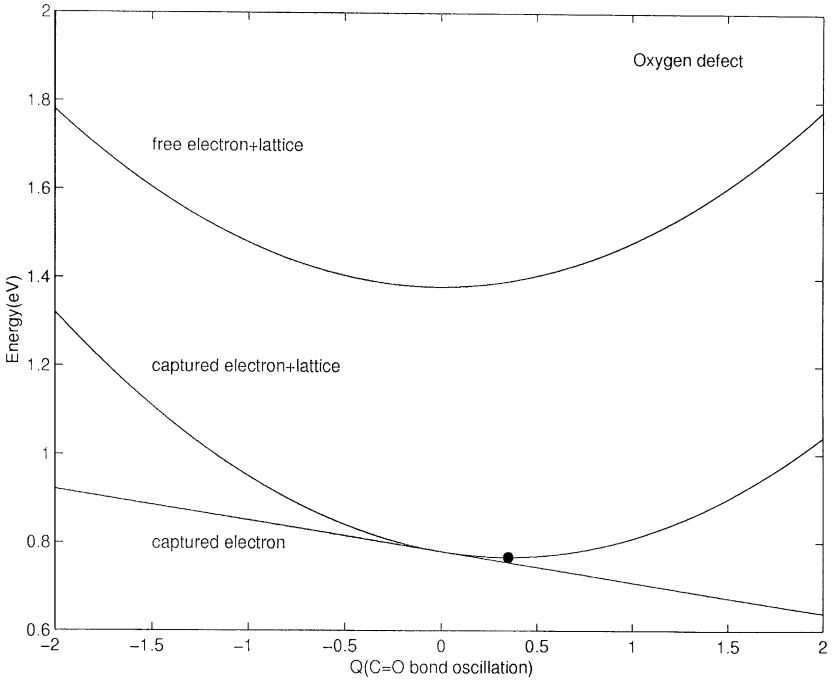

Fig. 8. The total energy E_t is the sum of lattice energy of the C = O bond and the electron energy is plotted as a function of the lattice displacement Q. The C = O bond is displaced to a new equilibrium position at $Q^* = 0.35$ (indicated by a dot), with new minimum total energy $E_t^* = 0.77$ eV, when the deep level is occupied by the electron.

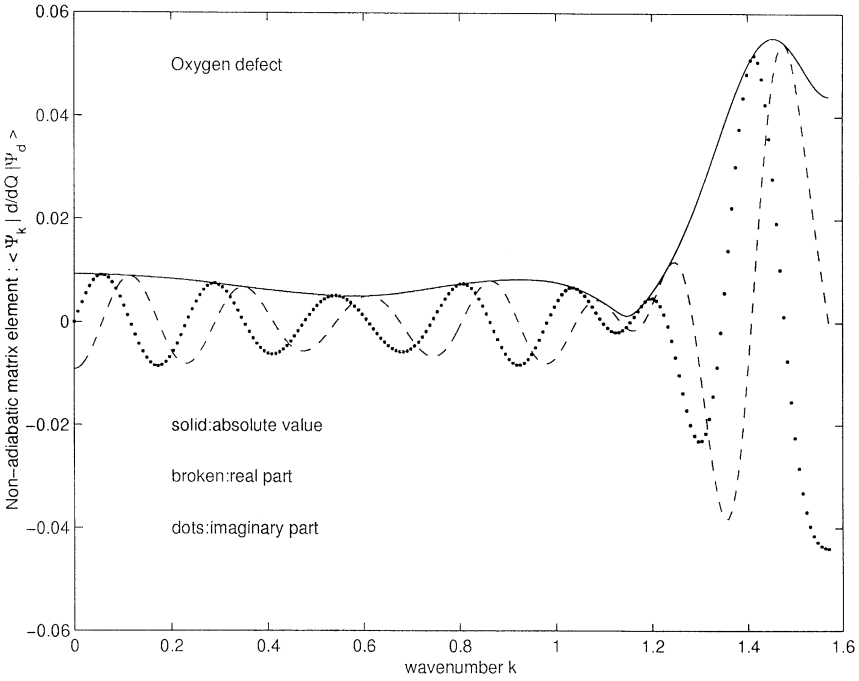

Fig. 9. The non adiabatic matrix element $\langle \Psi_k | d/dQ | \Psi_d \rangle$, obtained by numerical differentiation of the defect wavefunction Ψ_d, is shown as a function of the wavenumber k of the band state Ψ_k.

conduction band is empty. The electron–hole pair excited states $|k,-k\rangle$ with zero total momentum is related to the ground state $|g\rangle$ by $|k,-k\rangle = a^{\dagger}_{c,k} a_{v,k} |g\rangle$, where k and $-k$ are the electron and hole momentum, respectively. $a^{\dagger}_{c(v),k}$ and $a_{c(v),k}$ are the creation and annihilation operators for the corresponding states. Such electron–hole pair states are however not the elementary excitation because the Hamiltonian has off-diagonal matrix elements among them [16]:

$$H_{kk'} \equiv \langle k', -k' | H | k, -k \rangle = [E_g + (E^+_k - E^-_k)]\delta_{k,k'} + V_{kk'}. \quad (29)$$

The Coulomb matrix element is given by

$$V_{kk'} = \frac{1}{2} \int d\mathbf{r}\, d\mathbf{r}' \psi^*_{c,k'}(\mathbf{r}) \psi^*_{v,k}(\mathbf{r}') \frac{e^2}{\kappa |\mathbf{r} - \mathbf{r}'|} \times \psi_{v,k'}(\mathbf{r}') \psi_{c,k}(\mathbf{r}), \quad (30)$$

where κ is the background dielectric constant for the π-electrons, and e is the electron charge. The exciton state $|\mathrm{ex}\rangle$ with zero total momentum is obtained by diagonalizing the matrix representation $H_{kk'}$ of H in the electron–hole pair subspace spanned by $|k,-k\rangle$. The exciton energy E_{ex} is the lowest eigenvalue of $H_{kk'}$, the corresponding eigenvector $\phi_{\mathrm{ex}}(k)$ is the exciton wavefunction. $|\mathrm{ex}\rangle$ is expanded by the electron–hole pair states

$$|\mathrm{ex}\rangle = \sum_k \phi_{\mathrm{ex}}(k) |k, -k\rangle. \quad (31)$$

E_{ex} is usually written as $E_g + 2E_c - E_B$, where $E_c = E^+_{\pi/2} = -E^+_{\pi/2} = |t_1 - t_2|$ is the conduction band edge and $2E_c$ is the bandgap. E_B is the exciton binding energy. The Coulomb matrix element $V_{kk'}$ in Eq. (30) is difficult to evaluate accurately. Besides, the suitable value for κ due to core level and σ-electron screening remain somewhat uncertain. The spin index and the exchange effect are also neglected here by considering only the singlet excitons. Even though intensive works have been devoted to the calculation of E_B and ϕ^1_{ex}, the results remain controversial. Since the main

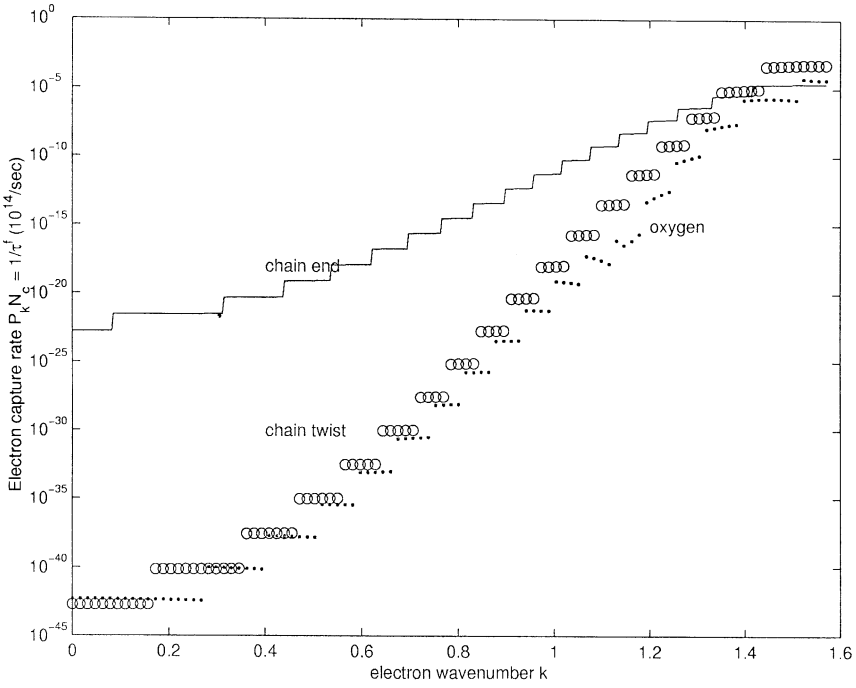

Fig. 10. The free electron capture rate $1/\tau^f$ when there is one defect per unit cell is shown as a function of the free electron wavenumber k. The result has to be multiplied by the defect density if it is not one.

purpose of this work is on the deep level defect within the SCF single-particle approximation, we do not calculate $V_{kk'}$, E_B and ϕ_{ex} here but use the results quoted from both the experimental and theoretical literature [2,6,24,25] for the calculation below.

Exciton in unstable against electron–hole dissociation when its energy E_{ex} is larger than the energy E_{dis} of the dissociated state with the electron in the deep level and the hole at top of the valence band. So we need to compare the two energies $E_{ex} = E_g + 2E_c - E_B$ and $E_{dis} = E_g + (E_d + E_c)$. E_d is the deep level energy at the relaxed lattice position Q^* calculated in Sections 2 and 3, measured from the middle of the bandgap which is E_c above the valence band top. The difference $E_{ex} - E_{dis}$ is $(E_c - E_d) - E_B$, where $E_c - E_d$ is the deep level binding energy. In other words, when the binding energy of the exciton is smaller than the binding energy of the deep level, the electron may drop into the level and the hole is released to the valence band to become a free charge carrier. The excess energy is carried away by the hole kinetic energy and the multi-phonon emission, as depicted in Fig. 11. This is similar to the capture process considered in Section 4, but now the initial state of the transition is $|ex; m\rangle$ and

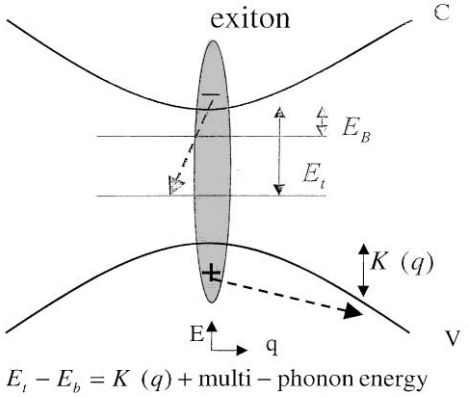

Fig. 11. When the deep trap level binding energy $E_t = E_c - E_d$ is larger than the exciton binding energy E_B, the exciton can dissociate into a trapped electron and a free hole with kinetic energy $K(q)$. The excess energy is carried away by the multi-phonon emission.

the final state is $|d,q;\,n\rangle$, where "ex" denotes exciton, d means defect for the electron and q is the Bloch state wavenumber of the hole. m,n are the occupation numbers of the local phonon mode. The total energy of the initial state is $E_{\rm ex}+\hbar\omega(m+1/2)$, while the total energy of the final state is $E_{\rm dis}+K(q)+\hbar\omega(n+1/2)$. $K\times(q)=E^{-}_{\pi/2}-E^{-}_{q}$ is the hole kinetic energy, where E^{-}_{q} is defined in Eq. (1). From energy conservation we have $(E_{\rm c}-E_{\rm d})-E_{\rm B}-K(q)=p\hbar\omega$, with $p=n-m$. $p\hbar\omega$ is the excess energy of the local lattice mode after the capture, which will be rapidly dissipated through the anharmonic coupling to the bulk phonon modes. The exciton capture rate $P_{\rm ex}$ is given by:

$$P_{\rm ex}={\rm Av}_m\sum_{q,n}|\langle d,q;\,n|H^{\rm NA}|{\rm ex};\,m\rangle|^2\times\delta[E_{\rm c}-E_{\rm d}-E_{\rm B}-K(q)-(n-m)\,\hbar\omega], \tag{32}$$

where the nonadiabatic matrix element is

$$\langle d,q;\,n|H^{\rm NA}|{\rm ex};\,m\rangle=\langle\Psi_{\rm d};\,\chi_n|H^{\rm NA}|\Psi_{-q};\,\chi_m\rangle\phi_{\rm ex}(q). \tag{33}$$

This is because the local phonon mode is only coupled to the electron, which is localized in the final state. The NA matrix element for the electron part is exactly the same as the free electron case calculated above. So the exciton quenching rate $P_{\rm ex}$ can be expressed as

$$\begin{aligned}P_{\rm ex}&=\sum_{q,n}|\phi_{\rm ex}(q)|^2{\rm Av}_m|\langle d;\,n|H^{\rm NA}|-q;\,m\rangle|^2\\&\quad\times\delta[E_{\rm c}-E_{\rm d}-E_{\rm B}-K(q)-(n-m)\hbar\omega]\\&=\sum_{q}|\phi_{\rm ex}(q)|^2P_q[p(q)]\theta[p(q)].\end{aligned} \tag{34}$$

Now the number of phonons p emitted is a function of the hole momentum $q:p(q)=[E_{\rm c}-E_{\rm d}-E_{\rm B}-K(q)]/\hbar\omega$. The step function in $P_{\rm ex}$ guarantees that the quenching occurs only when the final state is indeed lower than the initial state in energy. In practice we take the exciton wavefunction $\phi_{\rm ex}(q)$ to be a Lorentzian with width $1/a_{\rm B}$, where $a_{\rm B}$ is the exciton Bohr radius. Similar to the case of free electron capture, we define the capture rate $1/\tau^{\rm ex}\equiv P_{\rm ex}N_{\rm c}$. $P_{\rm ex}$ is in general larger than $P_{\pi/2}$, i.e. free carrier capture at the band edge, because of the exciton binding energy reduces the electronic energy difference $E_{\rm c}-E_{\rm B}-E_{\rm d}(Q^*)=p\hbar\omega$, resulting in a smaller p.

Combining Eqs. (20) and (34) and using the results in Fig. 10, we find $1/\tau_{\rm ex}$ is equal to 4.5 $\rm ns^{-1}$ for chain end, 3.6×10^2 $\rm ns^{-1}$ for oxygen. For chain twist, the defect energy $E_{\rm d}$ is below the exciton energy $E_{\rm ex}$ only when the twist angle θ is larger than 60°. For $60^\circ<\theta<75^\circ$, the exciton quenching rate is larger than that of the oxygen defect [19]. For $\theta>75^\circ$, the twist quenching rate is smaller than the oxygen defect. In particular, $1/\tau_{\rm ex}$ is equal to 3.2×10^3 $\rm ns^{-1}$ for $\theta=67.5^\circ$. We choose $E_{\rm B}=0.3$ eV [2,6] and $a_{\rm B}=5a$ [24,25], where a is the lattice constant.

6. Photoconductivity quantum yield

Under an incident photon flux $I_{\rm p}$, the steady state exciton number per unit cell $n_{\rm ex}$ and the defect filling fraction f satisfy the equilibrium conditions [19]

$$\begin{aligned}&\alpha_p vI_p-\frac{1}{\tau_r}n_{\rm ex}-\frac{1}{\tau_{\rm ex}}n_{\rm d}(1-f)n_{\rm ex}=0,\\&\frac{1}{\tau_{\rm ex}}n_{\rm ex}(1-f)-\frac{1}{\tau_2}f^2n_{\rm d}=0,\end{aligned} \tag{35}$$

where α_p is the absorption coefficient, v is the unit cell volume, and $\tau_{\rm r}$ is the radiative lifetime of the exciton. The free hole capture rate $1/\tau_2$ is taken as an adjustable parameter. The first equation is obviously the condition that the exciton generation and decay rate must be equal in equilibrium. The second equation will be more transparent if it is written as $(1/\tau_{\rm ex})n_{\rm ex}[(1-f)n_{\rm d}]-(1/\tau_2)(fn_{\rm d})(fn_{\rm d})=0$. The first term on the left-hand side is the free hole generation rate through exciton quenching, which is proportional to both the exciton density $n_{\rm ex}$ and the empty defect density $(1-f)n_{\rm d}$. The second term is the free hole capture rate, which is proportional to the filled defect density and the free hole density. Both of them are equal to $fn_{\rm d}$ in our model, because all holes come from the filling of defects by exciton quenching. In equilibrium these two terms must be equal. The steady state carrier generation quantum yield ζ is defined as the

ratio between the photon absorption rate and the carrier generation rate:

$$\zeta = \frac{n_d(1-f)n_{ex}/\tau_{ex}}{\alpha_p I_p v} = \frac{(1-f)n_d/\tau_{ex}}{(1-f)n_d/\tau_{ex} + 1/\tau_r}, \quad (36)$$

which is, of course, equal to the ratio between the exciton quenching rate and the total decay rate. The quantum yield decreases with the pumping intensity due to the deep level saturation by the pump. The results are shown in Fig. 12. When the pumping is so low that the filling of the defect level becomes negligible, the quantum yield ζ becomes $(n_d/\tau_{ex})/(n_d/\tau_{ex} + 1/\tau_r)$.

7. Discussion and conclusion

Based on the above results, we predict that the photoluminescence quantum yield is reduced to about one-half when there is one oxygen defect per 400 unit cells. Moreover, the PC quantum yield ζ caused by the structure defects (chain ends) is predicted to be 8.9×10^{-4} when the average number of unit cells N_c in a chain is at a typical value of 5×10^3. Our predictions on the relation between the PC quantum yields with the oxygen density (for oxidized samples) and with the chain length (for pristine samples) have been quantitatively compared with experiments [19], and the results are reasonable. The interpretation of the temperature (T) and electric field (E) dependence of the steady state photocurrent density $j(T, E)$ is now clear. Assuming that singlet excitons are generated with quantum yield close to one [26], j can be expressed as $j(E, T) = I_p \alpha_p d \zeta_t(T, E)\kappa(E, T)$. ζ_t is the total carrier generation quantum yield, including activation and the defect dissociation. κ is the collection efficiency by the electrode, and d is the film thickness. ζ_t can be written as $\zeta + be^{-\beta E_b}$, where ζ is the defect part and $be^{-\beta E_b}$ is the activated dissociation part. The T-dependence of ζ_t comes mainly from the activation part, while the T-dependence of κ comes from the activation from the traps along the passage to the electrodes. For

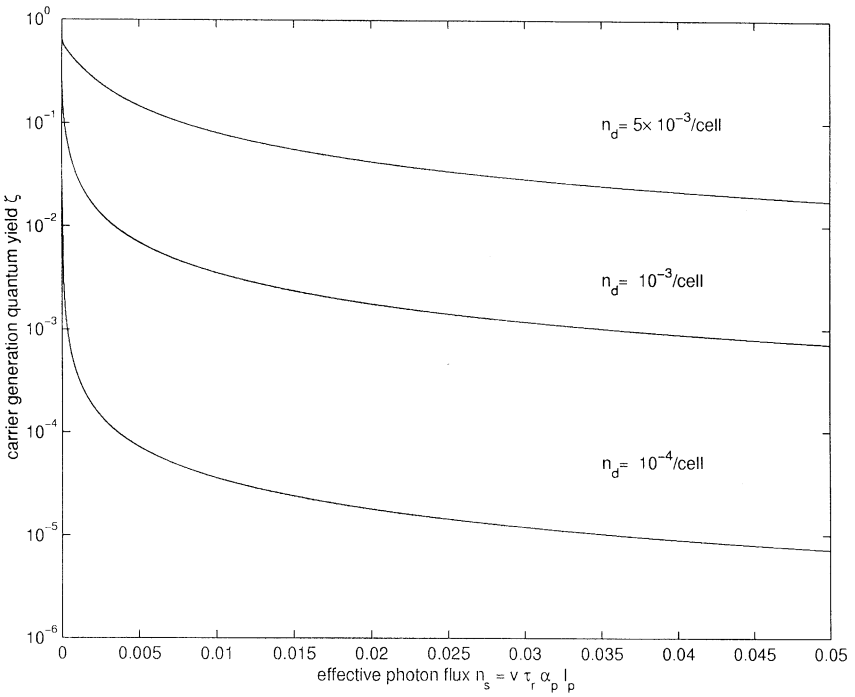

Fig. 12. The steady state quantum yield ζ is shown as function of n_s, which is proportional to the photon flux, for three defect levels. v is the unit cell volume. n_s would be the number of excitons per unit cell under photon flux I_p if there were no nonradiative channels.

thin films in the sweep-out region, the collection efficiency κ is close to one [26], so we have $j = I_p\alpha_p\zeta_t$ and j should be proportional to $\zeta + be^{-\beta E_b}$. The weak T-dependence in this situation implies that $be^{-\beta E_b} \ll \zeta$. This is no surprise because ζ has been estimated to be about 10^{-3} even without oxygen, while the factor $e^{-\beta E_b}$ is only 1.24×10^{-6} at 300 K. The "intrinsic" photocurrent of pure samples is therefore not mainly determined by the intrinsic properties of a perfect chain-like exciton binding energy, but by extrinsic factors including the defect density and the strength of the coupling between the lattice and the deep level. In thicker films the T-dependence of j is dominated by the transport factor κ instead of the generation factor ζ_t, as suggested by Moses et al. [4].

The multi-phonon exciton quenching rate depends on the exciton creation energy E_{ex} and the bandgap E_g. Unfortunately the value for E_g remains widely controversial, ranging from 2.8 to 3.4 eV [1–3]. In order for the quenching process to happen, the deep level energy E_d must lie below the exciton energy E_{ex}, which is experimentally determined to be 2.4 eV. For the case of chain end, E_d is fixed at the mid-gap value of $E_g/2$. So the energy requirement is always satisfied for all the above range of E_g. On the other hand, the deep level for the carbonyl group is found to be 0.6 eV (Fig. 8) below the conduction band edge, so the quenching process is possible only when E_g is below 3.0 eV. The carbonyl group has been observed to significantly increase the photoconductivity, so it can be considered as an experimental constraint that the defect level associated with oxygen must be deep enough to lie below the exciton energy, which is the situation we considered in this work.

Certain factors are not considered here, including, for example, the exciton quenching via the Auger process, the accurate account of the coupling between the local phonon mode and the electron level through the modulation of more than one bond, the scattering and cascade recapture of free holes by the trapped electron, and the interaction among the defects. Besides, in the rate equation we assumed that there is only one kind of deep level simultaneously responsible for the exciton quenching and free hole capture after generation. In practice, they may result from different traps with different energies. The many-body Coulomb interaction is believed to be strong in conjugated polymers [27]. It is, however, not included in our calculation explicitly, but taken into account by using the renormalized hoping integrals and other parameters to reproduce the self-consistent single particle spectrum. For the ground state, single particle levels below the Fermi level are filled. For the excited state (exciton), the Coulomb interaction has been included by properly choosing the exciton binding energy and wavefunction.

In conclusion, the exciton dissociation rates through deep levels due to oxidation and structure defects are calculated. The results agree with the experiments on the PC enhancement and PL quenching by oxidation. Moreover, even without oxygen the mid-gap level at the chain end causes a carrier generation rate larger than the thermal dissociation rate. So the main carrier generation process is not the thermal activation or field dissociation, but the relaxation through deep level traps. The "intrinsic" photocurrent is therefore disorder sensitive and not primarily determined by the intrinsic properties of a perfect chain. Our study clarifies the molecular exciton vs. semiconductor band controversy on the origin of photoconductivity in conjugated polymers.

Acknowledgements

We are grateful to H.H. Lin and C.Y. Mou for useful discussions, and thank the National Center for Theoretical Sciences of Taiwan, ROC for its hospitality. This work is supported by the National Science Council of Taiwan, ROC under contract Nos. 88-2112-M-009-006 (HFM), 88-2112-M-007-010 (TMH), and 89-2112-M-007-025 (TMH).

References

[1] N. Sariciftci (Ed.), Primary Photoexcitations in Conjugated Polymers: Molecular Exciton Versus Semiconductor Band Model, World Scientific, Singapore, 1997.

[2] S. Alvarado, P. Seidler, Phys. Rev. Lett. 81 (1998) 1082.
[3] M. Rohlfing, S. Louie, Phys. Rev. Lett. 82 (1999) 1959.
[4] D. Moses, J. Wang, G. Yu, A. Heeger, Phys. Rev. Lett. 80 (1998) 2685.
[5] D. Moses, H. Okumoto, C. Lee, A. Heeger, Phys. Rev. B 54 (1996) 4748.
[6] S. Barth, H. Bässler, Phys. Rev. Lett. 79 (1998) 4445.
[7] S. Barth, H. Bässler, H. Rost, H. Hörhold, Phys. Rev. B 56 (1997) 3844.
[8] H. Antoniadis, L. Rothberg, F. Papadimitrakopoulos, M. Yan, M. Galvin, M. Abkowitz, Phys. Rev. B 50 (1994) 14911.
[9] M. Yan, L. Rothberg, F. Papadimitrakopoulos, M. Galvin, T. Miller, Phys. Rev. Lett. 73 (1994) 744.
[10] L. Onsager, Phys. Rev. 54 (1938) 554.
[11] M. Chandross, S. Mazumdar, S. Jeglinski, X. Wei, Z. Vardeny, E. Kwock, T. Miller, Phys. Rev. B 50 (1994) 14702.
[12] N. Greenham, R. Friend, in: H. Ehrenreich, F. Spaepen (Eds.), Solid State Physics, Vol. 49, Academic Press, San Diego, 1995, p. 30.
[13] S. Brazovskii, N. Kirova, JETP Lett. 33 (1981) 4.
[14] F. Papadimitrakopoulos, K. Konstadinidis, T. Miller, R. Opila, Chem. Mater. 6 (1994) 1563.
[15] L. Rothberg, M. Yan, A. Fung, T. Jedju, E. Kwock, M. Galvin, Synth. Met. 84 (1997) 537.
[16] A. Szabo, N. Ostlund, Modern Quantum Chemistry: Introduction to Advanced Electronic Structure Theory, McGraw Hill, New York, 1989.
[17] W. Su, J. Schrieffer, A. Heeger, Phys. Rev. B 22 (1980) 2099.
[18] J.M. Ziman, Principles of the Theory of Solids, Cambridge, London, 1964.
[19] H.F. Meng, T.M. Hong, Phys. Rev. B 61 (2000) 9913.
[20] B.K. Ridley, Quantum Processes in Semiconductors, Oxford, New York, 1988.
[21] M. Lannoo, J. Bourgoin, Point Defects in Semiconductors, Springer, Berlin, 1981.
[22] C.A. Coulson, B. O'Leary, R.B. Mallion, Hückel Theory for Organic Chemists, Academic Press, London, 1978.
[23] E. Conwell, Phys. Rev. B 57 (1998) R12670.
[24] S. Abe, J. Yu, W.P. Su, Phys. Rev. B 45 (1992) 8264.
[25] P. Gomes da Costa, E. Conwell, Phys. Rev. B 48 (1993) 1993.
[26] N. Greeham, I. Samuel, G. Hayes, R. Phillips, Y. Kessener, S. Moratti, A. Holmes, R. Friend, Phys. Lett. 241 (1995) 89.
[27] D. Baeriswyl, D. Campbell, S. Mazumdar, in: H. Kiess (Ed.), Conjugated Conducting Polymers, Springer, Berlin, 1992.